RESEARCH ARTICLE | JULY 21 2023

Increased toughness and low cycle fatigue in ASSAB 709 m steel through normalizing process FREE

Helmy Alian ✉; Nukman; M. Badaruddin; Agung Mataram; Arief Mulya

AIP Conference Proceedings 2689, 070044 (2023)
https://doi.org/10.1063/5.0130326

Increased Toughness and Low Cycle Fatigue in ASSAB 709 M Steel Through Normalizing Process

Helmy Alian[1, a)], Nukman[1], M. Badaruddin[2], Agung Mataram[1] and Arief Mulya[1]

[1]*Department of Mechanical Engineering, Sriwijaya University, Indralaya, South Sumatera, 30662, Indonesia*
[2]*Department of Mechanical Engineering, Lampung University, Jalan Prof. S. Brojonegoro No.1, Bandar Lampung 35145, Indonesia*

[a)] *Corresponding author: helmyalian@ft.unsri.ac.id*

Abstract. The toughness and low cycle fatigue (LCF) resistance of ASSAB 709 M steel before and after normalizing were investigated at room temperature. The normalizing process causes an increase in plastic energy and ductility but decreases mechanical strength. The normalizing treatment of ASSAB 709 M steel improves the LCF resistance and impact energy of the material. Also, increasing strain amplitude indicates the transition behaviour from initial cyclic softening to stable cyclic hardening. On the other hand, ASSAB 709 M steel, before normalizing, undergoes progressive cyclic softening until it fails. The ASSAB 709 M steel microstructure changes after normalizing from the amount of martensite lath to the formation of pearlite and ferrite. These microstructural changes cause behavioural changes at low and high strain amplitudes due to the normalizing process. The enhancement of the low cycle fatigue resistance of the annealed steel is attributed to the high magnitude of the compressive stress, dependent on the applied strain amplitude.

INTRODUCTION

ASSAB 709 M steel contains ~ 0.4 wt.% carbon is classified as low-alloy commercial steel widely applied to engine components that experience great stress, such as connecting rods, gears, spindles, pinions, pump shafts, ring gear, and others. Therefore, this steel must have sufficient ductility, toughness, and resistance to low cycle fatigue during its application. The conventional production of ASSAB 709 M steel uses the quenching and tempering (Q&T) method, which generally produces a tempered martensite phase [1,2]. However, the Q&T combination process increases the ductility and toughness of steel but inevitably has to sacrifice the magnitude of the ratio of yield strength and maximum strength of steel [3,4].

Limited raw materials, production costs and costs to meet these needs are the main reasons researchers have developed several technical methods to increase material life, such as nitriding [5,6], carburizing [7] and shot peening [8]. However, the application of this method can cause high strain hardening in the surface area of the steel and contribute to distortion, which leads to decreased ductility of the steel.

To improve the fatigue properties of AISI 4140 steel, the ratio of plastic and elastic energy must be greater, and the annealing process of AISI 4140 steel at a strain amplitude of 0.3% increases the fatigue life of steel by 2.4 times [9]. However, even though the fatigue life increased, the strength of the steel decreased by almost 40%.

There are several ways to obtain high strength ASSAB 709 M steel with a large ductility and relatively low ratio, namely through grain engineering and inserting the soft ferrite phase into the martensite microstructure without being tempered produce the bainite phase [10]. One advanced method is the austempering process, but it has not significantly improved fatigue resistance [11]. The microstructure significantly affects the rate of growth that takes back fatigue and thresholds [8]. Several researchers have become more interested in developing the austempering process for AISI 4140 steel as a traditional heat treatment process: austenitizing, quenching and tempering. Steel with a carbon content of about 0.40% can produce the same strength as steel produced from the Q&T process, but the fracture toughness is still not good [12]. Research through the austempering process on ASSAB 709 M steel has been carried out to produce a fairly high strength but very low increase in fatigue resistance [13].

Toward Adaptive Research and Technology Development for Future Life
AIP Conf. Proc. 2689, 070044-1–070044-10; https://doi.org/10.1063/5.0130326
Published by AIP Publishing. 978-0-7354-4470-6/$30.00

The purpose of this research is to increase the toughness and low-cycle fatigue resistance of ASSAB 709 M steel through the normalizing process, which later has high ductility so that it can be used in various applications of structural components that experience low-cycle fatigue loads.

EXPRIMENTAL PROCEDURES

Materials and Specimens

The test specimens of ASSAB 709 M were made using CNC following the standard machine/equipment to be used, namely tensile test (ASTM E8), fatigue test (ASTM E 606) and impact test (JIS Z2202).

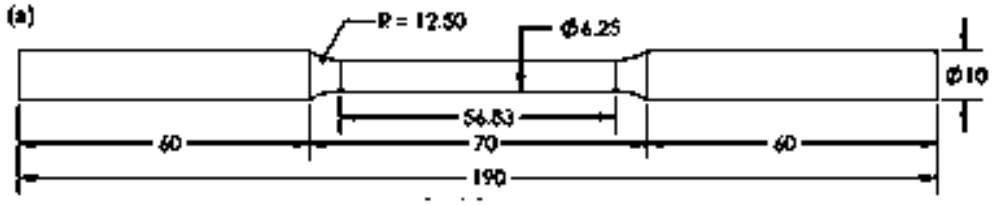

FIGURE 1. Tensile test specimen (ASTM E8)

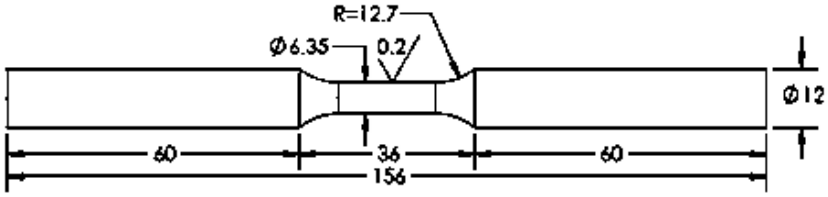

FIGURE 2. Specimen low cycle fatigue (ASTM E606)

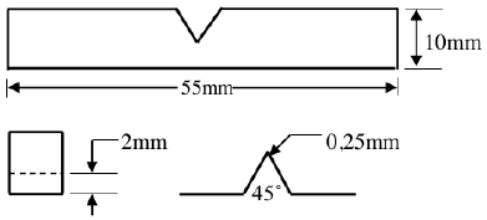

FIGURE3. Impact specimen (JIS Z2202)

Normalizing Process

This process normalizes the heat treatment process by heating the steel in the furnace to an austenitizing temperature of 850° C with a holding time of 60 minutes then cooled in the air.

Experiments

Mechanical properties including tensile strength, elongation, reduction in cross-sectional area, Charpy impact energy are measured using the average of three experimental results for each heat-treatment process. The composition test results are used to determine the temperature of austenitization using the Bhadeshia software algorithm and will also be seen in the Fe3-C equilibrium phase diagram. Static and low cycle fatigue testing uses the MTS Landmark 100 kN engine (static and dynamic) version of the latest released material fatigue test equipment

from MTS USA. Impact testing on specimens before and after normalizing was carried out using the Carpy impact machine.

Microstructure observations were made on specimens before and after the normalizing process etched with 2% Nital solution to reveal microstructure observations under an optical microscope: Measuring Microscope STM6-LM. Fractographical observation to see the fracture on the impact test fracture and low cycle fatigue using Scanning Electron Microscopy (SEM).

FIGURE 4. 100 kN MTS Landmark engine

RESULTS AND DISCUSSION

In this study, the data obtained were based on the average test of three specimens for each research variable.

Chemical Composition Testing

The specimen material was ASSAB 709 M steel, tested for chemical composition shown in Table 1. The composition test results are used to determine the austenitization temperature using the Bhadeshia software algorithm used for the normalizing process.

TABLE 1. Chemical composition of ASSAB 709 M steel

Element	Composition (%)	Element	Composition (%)
C	0,442	W	0,0077
Si	0,293	Pb	<0,002
Mn	0,739	Sn	0,00079
P	0,0135	Mg	<0,001
S	0,0042	As	0,003
Cr	1,06	Zr	0,0042
Mo	0,169	Bi	0,0044
Ni	0,0506	Ca	0,00058
Al	0,0153	Ce	0,0071
Co	0,0086	Te	0,0026
Cu	0,0133	Ta	0,0686
Nb	<0,004	Zn	00034
Ti	0,0249	La	0,0018
V	<0,0005	Fe	97

Tensile Testing

The results of the tensile test using the MTS Landmark 100 kN engine are as follows.

TABLE 2. Tensile test results of ASSAB 709 M

Material	σ_y (MPa)	σ_{ult} (MPa)	E_e (kJ)	E_p (kJ)	e (%)
Before normalizing	735,442	1097,858	0,085	0,003	21,406
After normalizing	658,957	916,785	0,087	0,002	23.358

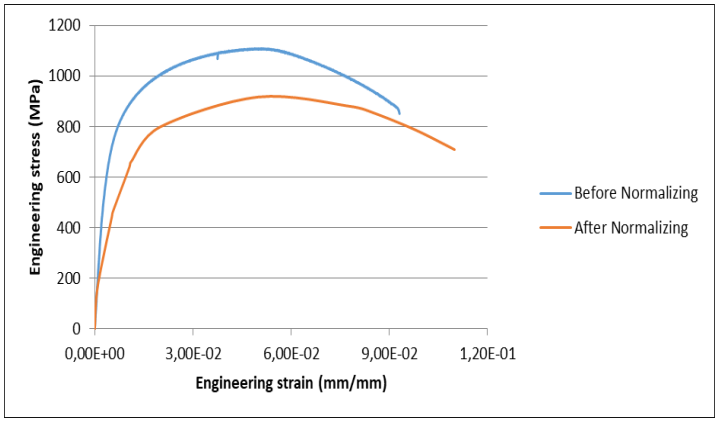

FIGURE 5. Stress vs strain curve of ASSAB 709 M steel before and after Normalizing

The stress-strain curves for ASSAB 709 M steel before and after normalizing are depicted in Fig. 5. Steel's modulus of elasticity (E) is determined by plotting a linear elastic curve with a line segment length of 20% in the range of the linear stress-strain relationship using the regression method. The yield strength, σ_y, is calculated using the 0.2% offset method. The results of the tensile test are summarized in Table 2. Although normalizing treatment of ASSAB 709 M steel reduces the mechanical strength, the ultimate strength (σ_{ult}), yield strength (σ_y) of the steel, ductility, and the energy of the plastic are significantly increased.

Low Cycle Fatigue Testing

The results of the tensile test using the MTS Landmark 100 kN engine are as follows.

TABLE 3. Results of low cycle fatigue test (LCF) of ASSAB 709 M steel before normalizing (BN) and after normalizing (AN)

Specimen	$\Delta\varepsilon_t$ (mm/mm)	ε_a(mm/mm)		E (GPa)	N_f (cycles)	σ_a (MPa)
		ε_{ap}	ε_{ae}			
BN-1	0.0035	0.00072	0.00728	207.4847	21490	559.50
BN-2	0.0050	0.00180	0.00320	207.0820	2454	633.00
BN-3	0.0065	0.00300	0.00350	208.7569	1385	687.00
BN-4	0.0080	0.00421	0.00379	208.2420	823	738.50
BN-5	0.0095	0.00546	0.00404	207.7356	357	776.50
BN-6	0.0110	0.00684	0.00416	207.8468	197	803.00
AN-1	0.0035	0.00150	0.00150	207.1000	26858	333.00
AN-2	0.0050	0.00310	0.00190	202.0700	3606	381.50
AN-3	0.0065	0.00490	0.00210	202.0600	1912	436.50
AN-4	0.0080	0.00660	0.00250	198.2700	733	464.50
AN-5	0.0095	0.00850	0.00250	200.2500	415	498.00
AN-6	0.0110	0.01050	0.00250	195.4600	336	516.50

The results of the LCF test are shown in Table 3. The average modulus of elasticity for ASSAB 709 M steel before and after normalizing was 200.87 GPa and 193.32 GPa, respectively. The effect of strain amplitude on the

cyclic stress response concerning the number of cycles at a constant strain rate is depicted for each steel in Fig. 6 (a) and (b). The peak stress of the ASSAB 709 M steel before normalizing increases with the strain amplitude (Fig. 6a). Conversely, it showed identical cyclic stresses at the higher strain amplitudes (Fig. 6(b)).

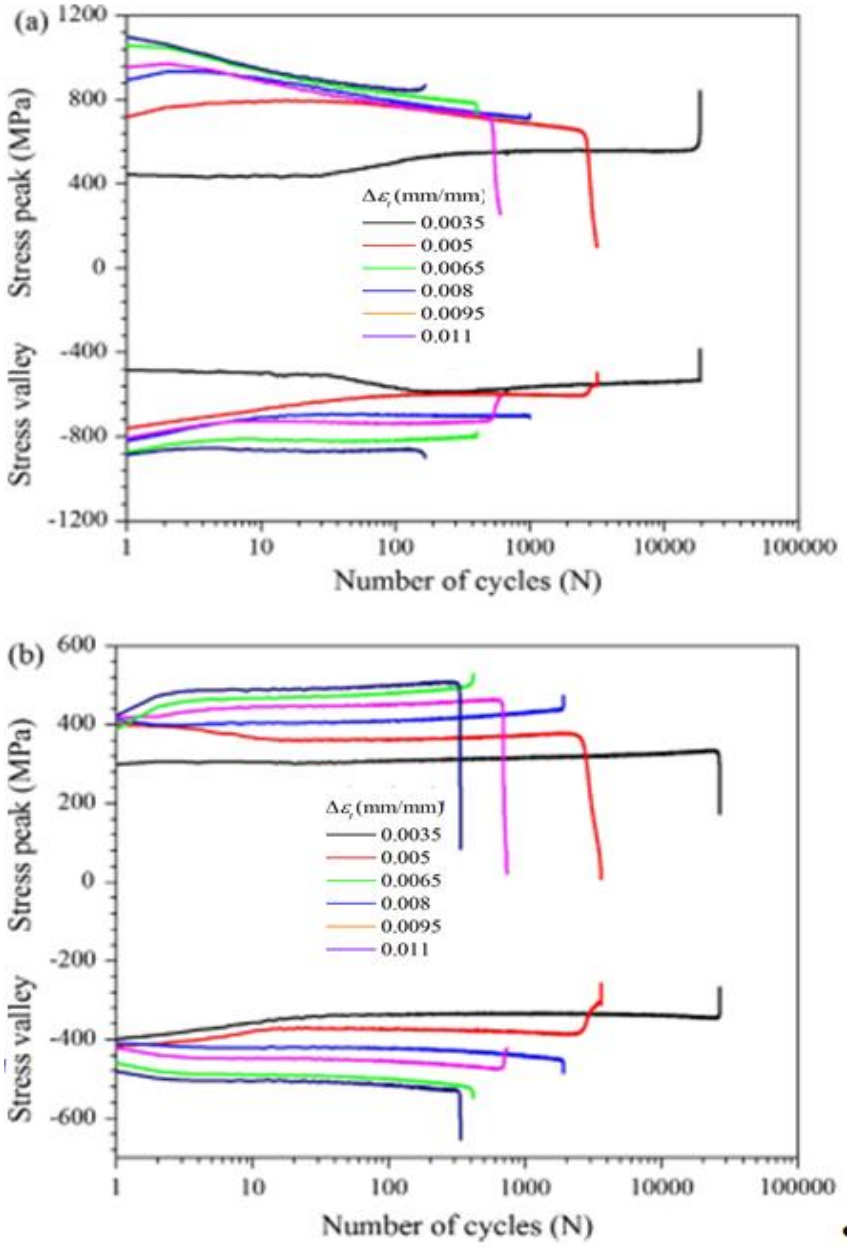

FIGURE 6. Cyclic voltage during low cycle fatigue testing: (a) before normalization (b) after normalization

At lower strain amplitudes, the difference in the response of cyclic stress to the peak (tensile) and valley (compressive) stresses of SN_1 specimens with TN_1 specimens is about 150 MPa and about 100 MPa. The TN_1 specimen showed a continuous mild cyclic softening behaviour for 30 cycles, and a progressive cyclic hardening behaviour was observed from 1000 cycles until the steel underwent cyclic saturation hardening and finally failed. In addition, a slight increase in the amount of compressive stress was observed from 1 to 1000 cycles. When the strain amplitude was increased (0.005-0.009 mm/mm), ASSAB 709 M before normalizing underwent an initial cyclic hardening for two cycles. Fig.6a clearly shows the initial cyclic hardening and continuous cyclic softening behaviour

of ASSAB 709 M steel without normalizing, which is highly correlated with the relatively high portion of martensite in the initial microstructure (Fig. 9). Similar behaviour is commonly found in many HSLA intermediate carbon sheets of steel, such as double-phase (ferrite-martensite) steels [10,12], CrMoV steels [14], and carbide-free bainitic steels [7,15,16], microstructures having more martensite phase rather than ferrite phase.

Impact Testing

The impact test method used in this test is the Charpy method with a rectangular cross-sectional area of 10x10 mm and a notch angle of V-45 with the notch position back from the pendulum's direction. The results of the impact test are processed with the following equation:

$$E_1 = P\ (D - D \cos \alpha) \quad (1)$$

$$E_2 = P\ (D - D \cos \theta) \quad (2)$$

$$E_{Tot} = E_1 - E_2 \quad (3)$$

Where:
E = Energy (joules)
P = hammer weight (25.68 kg) = (25.68 kg x 9.8 m / s = 251,921)
D = Pendulum diameter (0.65)
Cos α = Hammer lift angle (100)
Cos θ = Angle of swing after hitting the specimen
A = Area under the notch (80 mm2)

TABLE 4. Impact test results

No.	Specimen	E (Joule)	W (Joule)	$E_{average}$ (Joule)	$W_{average}$ (Joule)
1.	BT	56.870	0.7108	51.253	0.6401
2.	BT	45.551	0.5693		
3.	BT	51.224	0.6403		
4.	AN	59.680	0.7460	56.856	0.7108
5.	AN	54.051	0.6756		
6.	AN	56.870	0.7110		

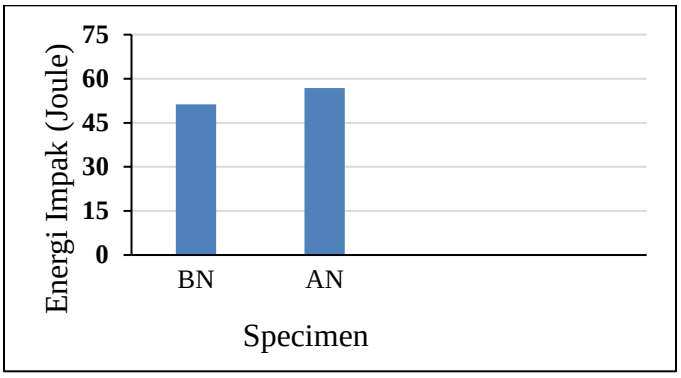

FIGURE 7. Graph of ASSAB 709 M steel impact energy before normalization (BN) and after normalization (AN)

From the results of the calculation of the impact test data in Table 4 and Fig. 7 above, there are differences in the toughness characteristics of ASSAB 709 M steel specimens before and after the normalization process, where the energy value increases from 51.253 to 56.856 Joules. This toughness increase is caused by the normalization process

in which the specimen is slowly cooled in air, increasing the ductility of the steel and the grain of the normalized specimen is finer than before normalization.

Microstructures

The area observed in this microstructure test is the surface of ASSAB 709 M steel before and after undergoing the normalizing process. The solution used to see the microstructure of carbon steel is 3% nital solution (with a composition of 3 ml of nitric acid and 97 ml of alcohol). Below are the results of microstructure testing on specimens that have been etched.

From the observations of the microstructure test above the microstructure of the specimen before normalizing, there is a martensite structure which proves that the ASSAB 709 M steel material used in this research has been carried out by a quenching process during production to increase the strength of the steel because it is widely used in the system construction.

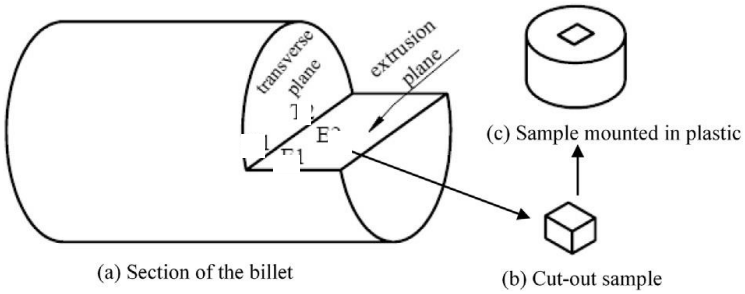

FIGURE 8. Annotation of the metallographic

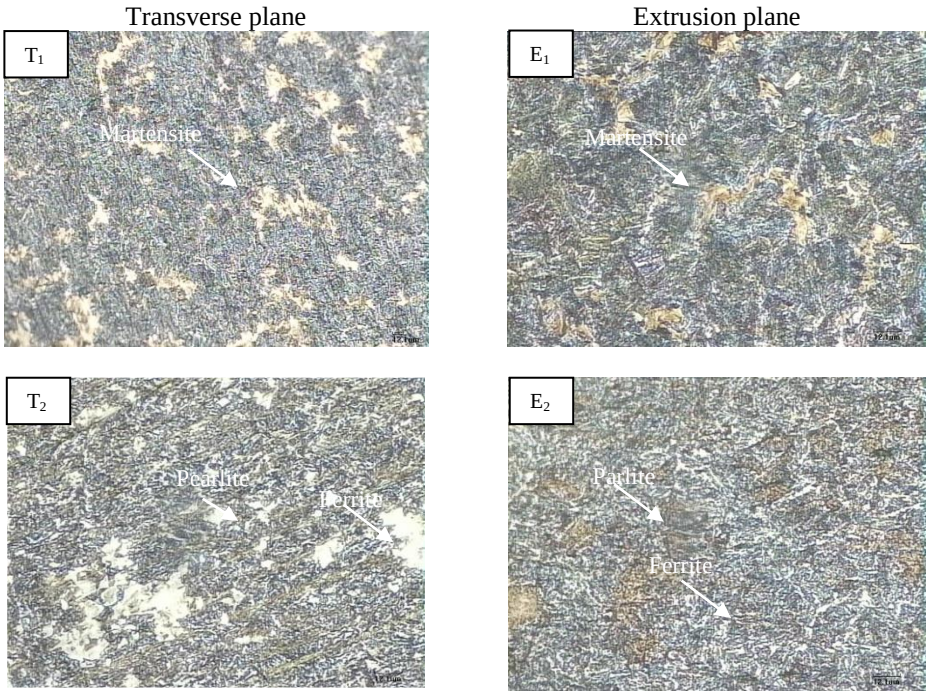

FIGURE 9. Optical micrograph of ASSAB 709 M steel in transverse and extrusion directions T1 and E1: before normalizing, T2 and E2 after normalizing

For the results of the observation of the microstructure test on specimens that have been carried out the normalization process, the austenite phase changes are then cooled by normalizing in the open air to room

temperature. From the microstructure results with the magnification of 500x, it was found that there was a phase change that occurred as a normalizing process result. The dominant phases of the microstructure above are ferrite and pearlite. Ferrite is lighter in colour because it has a low carbon content. Ferrite is soft and ductile. Although pearlite is darker in colour, it contains more carbon content than ferrite. Pearlite is strong and hard. The microstructural changes caused by heat treatment of ASSAB 709 M steel (Fig. 9) significantly affect the mechanical strength of the steel, the ductility of ferrite will increase the ductility of ASSAB 709 M steel.

The 0.442% carbon mass fraction in ASSAB 709 M steel is more than sufficient to produce a large martensite volume via the interstitial carbon atoms in body-centred tetragonal martensite (BCT), which results in more martensite particles. In the form of a solid solution in the ferrite matrix. In addition, small Fe3C particles which precipitate in the martensite phase can strengthen ferrite [11,15]. The small ferrite grains and the fine martensite dispersion (Fig. 9) provide a large ferrite-martensite phase boundary area. Thus, the available phase boundary area can serve as a barrier to the movement of the dislocation, substantially increasing the strength. Additionally, as shown in Fig. 9, the relative thickness of the ferrite layer in the microstructure is one of the reasons for the relatively high ductility of the normalized steel.

Fractographical Observation

SEM Fractography of Fig. 10(a) and (b) displays the typical surface fracture of the Low Cycle Fatigue (LCF) tested specimen, showing spherical and cementitious lamellae particles within the fracture surface near the surface (with dashed waves). Spherical cementite particles with carbon can act as a barrier to dislocation movement, contributing to early cyclic hardening for several cycles at low strain amplitudes. However, cementite balls that are well-known randomly in the small cluster region cannot effectively resist complex dislocation motion during strain cyclic deformation [12]. In addition, the small localized plastic strain and high-stress concentration in the martensite phase are believed to cause the rapid formation of microcracks [13]; thus, many sub-cracks are formed at the ferrite-martensite boundary, as shown in Fig. 10(c) and (d), which accelerate crack propagation.

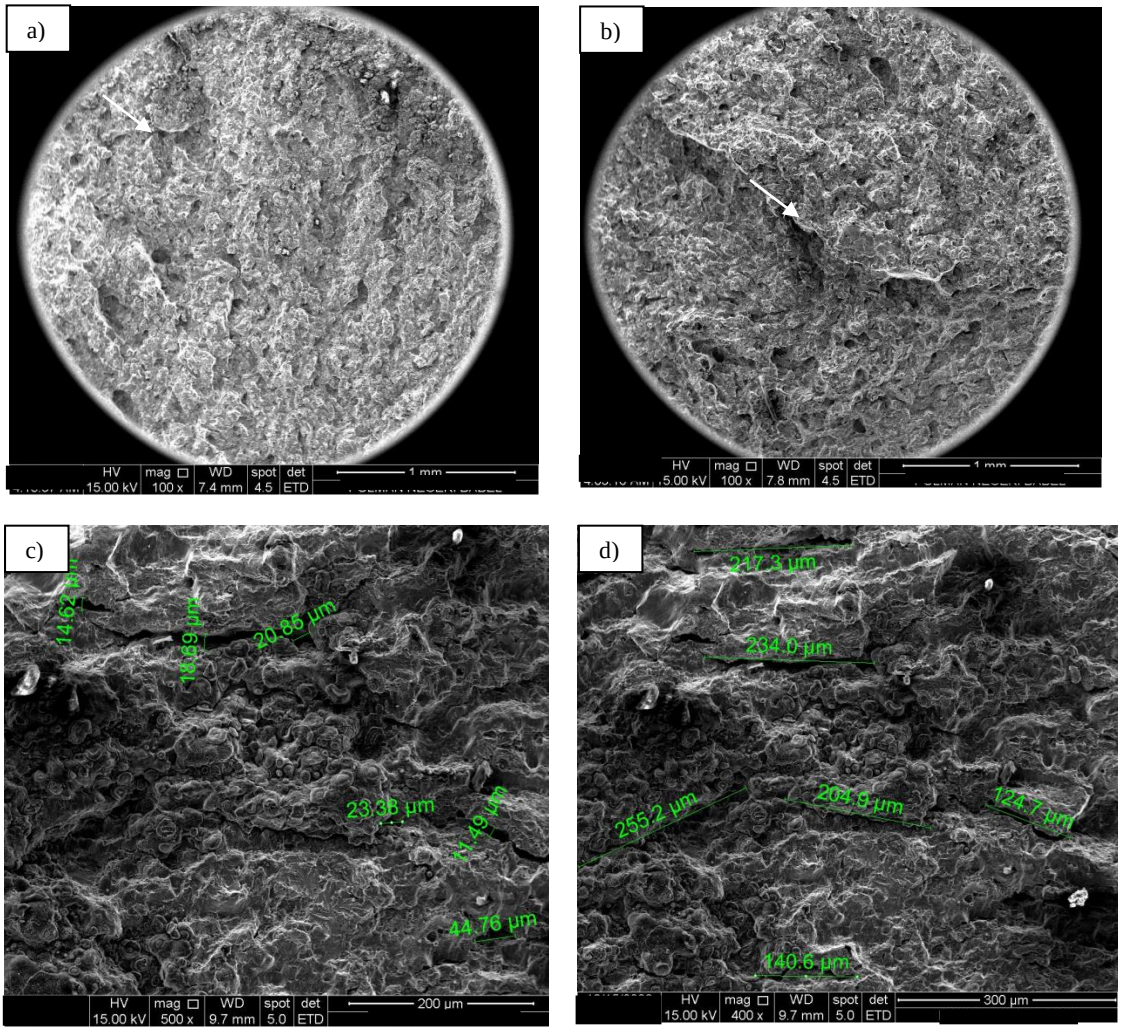

FIGURE 10. Surface fracture after LCF of ASSAB 709 M steel

Furthermore, features such as cleavage facets caused by the cleavage of the hard martensite phase and the risk of slipping of the soft ferrite phase during cyclic strain bodies can be seen in the fatigue propagation zone. The second phase is particle inclusion, where the cracks start and spread due to the relatively weak bonding of the particles to the matrix [13,15].

CONCLUSION

Based on the data and discussion above, it can be concluded that:

1. Based on the chemical composition of ASSAB 709 M steel, the proportion other than Fe <15%, this steel is classified as low-solid steel and based on its carbon content percentage of 0.442%, ASSAB 709 M steel is classified as medium carbon steel.
2. After the normalisation process, the ductility of ASSAB 709 M steel has increased, but its strength has decreased.
3. Low cycle fatigue resistance (Low Cycle Fatigue) after the normalization process has increased significantly.
4. The impact energy increased from ASSAB 709 M steel which was normalized compared to the one without normalization.

5. The microstructure of ASSAB 709 M steel has changed after normalization, before normalizing the amount of martensite lath and after normalizing pearlite and ferrite formed.
6. Many sub-cracks are formed at the ferrite-martensite boundary, as shown in Fig. 11(c) and (d), which accelerate crack propagation.

REFERENCES

1. Meysami AH, Ghasemzadeh R, Seyedein SH, Aboutalebi MR. An investigation on the microstructure and mechanical properties of direct-quenched and tempered AISI 4140 steel. Mater Des. 2010;31(3):1570–5.
2. Sanij MHK, Banadkouki SSG, Mashreghi AR, Moshrefifar M. The effect of single and double quenching and tempering heat treatments on the microstructure and mechanical properties of AISI 4140 steel. Mater Des. 2012;42:339–46.
3. De Cooman BC. Structure–properties relationship in TRIP steels containing carbide-free bainite. Curr Opin Solid State Mater Sci. 2004;8(3–4):285–303.
4. Zou Y, Xu YB, Hu ZP, Gu XL, Peng F, Tan XD, Chen SQ, Han DT, Misra RDK, Wang GD. Austenite stability and its effect on the toughness of a high strength ultra-low carbon medium manganese steel plate. Mater Sci Eng A. 2016;675:153–63.
5. Kovacı H, Yetim AF, Baran Ö, Çelik A. Fatigue crack growth analysis of plasma nitrided AISI 4140 low-alloy steel: part 2-variable amplitude loading and load interactions. Mater Sci Eng A. 2016;672:265–75.
6. Şengül AB, Çelik A. Effect of plasma nitriding on fatigue crack growth on AISI 4140 steel under variable amplitude loading. Surf Coatings Technol. 2011;205(21–22):5172–7.
7. Nagarajan VR, Putatunda SK, Boileau J. Fatigue crack growth behavior of austempered AISI 4140 steel with dissolved hydrogen. Metals (Basel). 2017;7(11):1–18.
8. Thielen PN, Fine ME, Fournelle RA. Cyclic stress strain relations and strain-controlled fatigue of 4140 steel. Acta Metall. 1976;24(1):1–10.
9. Boniardi M, D'Errico F, Tagliabue C. Influence of carburizing and nitriding on failure of gears–A case study. Eng Fail Anal. 2006;13(3):312–39.
10. Ye C, Suslov S, Kim BJ, Stach EA, Cheng GJ. Fatigue performance improvement in AISI 4140 steel by dynamic strain aging and dynamic precipitation during warm laser shock peening. Acta Mater. 2011;59(3):1014–25.
11. Paul SK, Stanford N, Hilditch T. Effect of martensite volume fraction on low cycle fatigue behaviour of dual phase steels: Experimental and microstructural investigation. Mater Sci Eng A. 2015;638:296–304.
12. Hwang B-C, Cao T-Y, Shin SY, Kim S-H, Lee S-H, Kim S-J. Effects of ferrite grain size and martensite volume fraction on dynamic deformation behaviour of 0· 15C–2· 0Mn–0· 2Si dual phase steels. Mater Sci Technol. 2005;21(8):967–75.
13. Tartaglia JM, Hayrynen KL. A comparison of fatigue properties of austempered versus quenched and tempered 4340 steel. J Mater Eng Perform. 2012;21(6):1008–24.
14. Badaruddin M, Kuncoro PS, Suudi A, Mesin JT, Teknik F, Lampung U, Lampung B. Low Cycle Fatigue Analysis of an Annealed AISI 4140 Steel. 2018;(1):56–61.
15. Jordon JB, Horstemeyer MF. Microstructure-sensitive fatigue modeling of AISI 4140 steel. J Eng Mater Technol. 2014;136(2):21004.
16. Bhadeshia HKDH. Materials Algorithms Project Program Library.